iScience

CellPress
OPEN ACCESS

Article

Dry molten globule conformational state of CYP11A1 (SCC) regulates the first step of steroidogenesis in the mitochondrial matrix

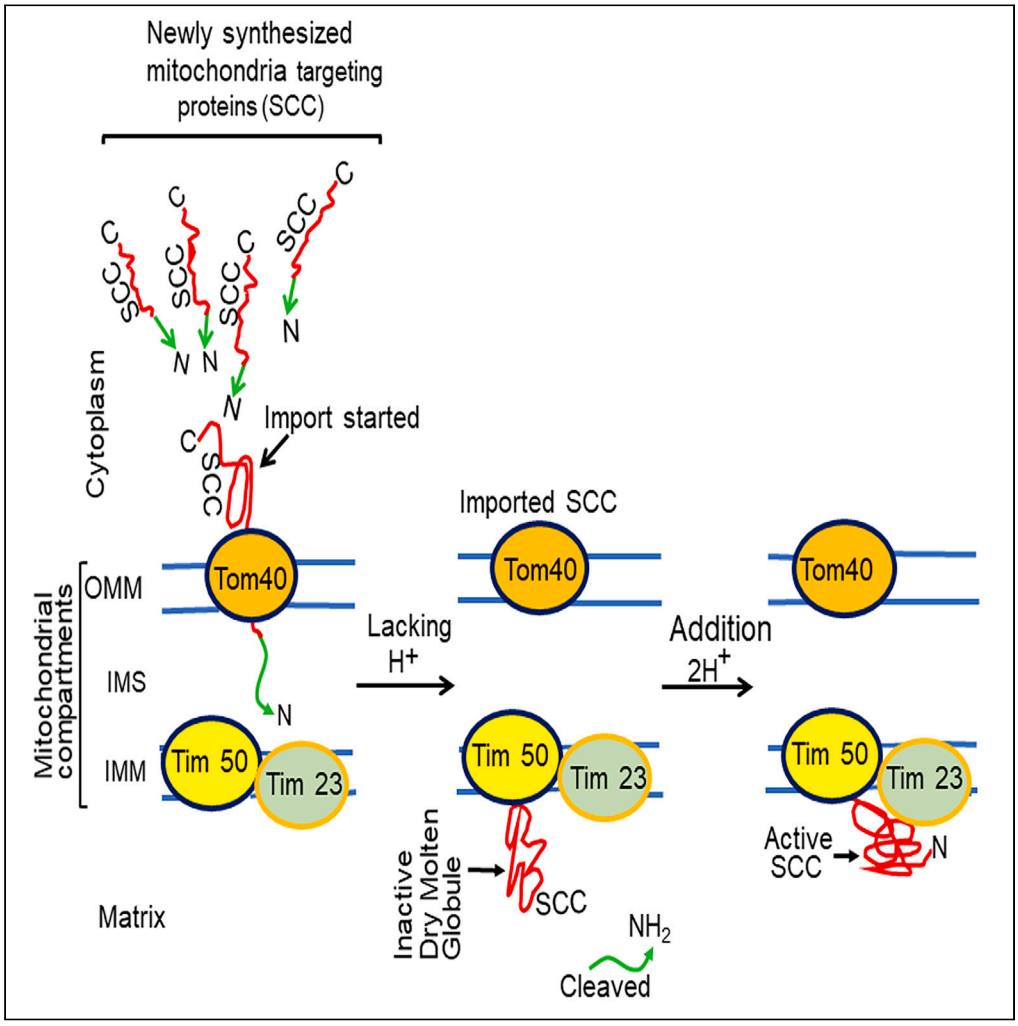

Himangshu S. Bose

bose_hs@mercer.edu

Highlights

CYP11A1 forms dry molten globule in the matrix

In vivo dry molten globule is a stable intermediate

Dry molten globule has limited interacting network

Dry to wet molten globule is steroidogenesis rate limiting step

Bose, iScience *27*, 110039
June 21, 2024
https://doi.org/10.1016/j.isci.2024.110039

iScience

CellPress
OPEN ACCESS

Article

Dry molten globule conformational state of CYP11A1 (SCC) regulates the first step of steroidogenesis in the mitochondrial matrix

Himangshu S. Bose[1,2,3,*]

SUMMARY

Multiple metabolic events occur in mitochondria. Mitochondrial protein translocation from the cytoplasm across compartments depends on the amino acid sequence within the precursor. At the mitochondria associated-ER membrane, misfolding of a mitochondrial targeted protein prior to import ablates metabolism. CYP11A1, cytochrome P450 cholesterol side chain cleavage enzyme (SCC), is imported from the cytoplasm to mitochondrial matrix catalyzing cholesterol to pregnenolone, an essential step for metabolic processes and mammalian survival. Multiple steps regulate the availability of an actively folded SCC; however, the mechanism is unknown. We identified that a dry molten globule state of SCC exists in the matrix by capturing intermediate protein folding steps dictated by its C-terminus. The intermediate dry molten globule state in the mitochondrial matrix of living cells is stable with a limited network of interaction and is inactive. The dry molten globule is activated with hydrogen ions availability, triggering cleavage of cholesterol sidechain, and initiating steroidogenesis.

INTRODUCTION

Multiple molecular metabolic processes occur in the mitochondria; therefore, its function is critical for mammalian survival. Mitochondria dysfunction increases with age in several organisms and with late-onset life-threatening diseases, including neurodegenerative disorders, cardiovascular diseases, endocrine diseases, and cancer.[1,2] Given the variety and severity of mitochondrial-associated diseases, preservation of mitochondrial function throughout aging has been a long-standing goal, with therapeutic efforts focusing mainly on the enhancement of mitochondrial biogenesis and quality control.[3]

Mitochondrial function requires a functional protein translocation system,[4] which mediates translocation of 99% of all mitochondrial proteins from the cytoplasm and is conserved from yeast to humans.[5] Mitochondrial protein import is determined by a specific amino acid sequence within the precursor called a signal sequence or targeting signal. The molecular basis of mitochondrial protein translocation initially depends on folding in the cytoplasm. At the outer mitochondrial membrane (OMM), any misfolding prior to import might generate clogging, and misfolding in the matrix might reduce or stop the metabolic process.[3] Therefore, precursor proteins must be in an unfolded or loosely folded conformation to allow their passage through tightly gated membrane pores.[6]

In adrenal and gonadal (ovary for women) tissues, steroidogenic acute regulatory protein (StAR) facilitates cholesterol transport from the outer to inner mitochondrial membrane (IMM) interacting with Tom40.[7,8] Next cytochrome P450 cholesterol side chain cleavage enzyme (CYP11A1/P450scc/SCC) catalyzes the conversion of cholesterol to pregnenolone in the matrix side followed by catalysis to progesterone by the inner mitochondrial space (IMS) resident protein 3-beta hydroxy steroid dehydrogenase-2 (3βHSD2).[9] New born babies with mutation in StAR[10] or SCC[11] or 3βHSD2 results in diminished production of cortisol and enlarged adrenal gland developing issues with salt-loosing crisis and gender identity problem.[12–14] Therefore, the first steroid pregnenolone is essential for the final synthesis of mineralocorticoids, glucocorticoids, and sex steroids, all of which are essential for electrolyte balance, stress management, and sexual differentiation.[15]

Cholesterol is the only substrate for pregnenolone synthesis in the mitochondria. Until all the newly transported cholesterol molecules are catalyzed by SCC, a new pool of cholesterol cannot be transported from the cytoplasm.[15,16] Lack of SCC activity would be incompatible with full-term gestation because the placenta, a fetal tissue, must produce progesterone from the second trimester for successful gestation.[13] During acute stress, immediate production of cortisol is necessary although it still requires approximately 20 min to be available.[17]

StAR transports cholesterol into mitochondria in a molten globule conformation.[18] Because in an active molten globule state, StAR remains in a compact intermediate state of folding at the OMM where the part of its tertiary structure was lost with no change in secondary structure.[18,19] Similarly, amino terminal truncated MLN64 (*N*-218 MLN64) transports 50% cholesterol from the cytoplasm to mitochondria in a molten globule conformation for SCC to catalyze to pregnenolone.[20,21] IMS resident 3βHSD2 is active in a molten globule state for

[1]Laboratory of Biochemistry, Biomedical Sciences, Mercer University School of Medicine, Savannah, GA 31404, USA
[2]Anderson Cancer Institute, Memorial University Medical Center, Savannah, GA 31404, USA
[3]Lead contact
*Correspondence: bose_hs@mercer.edu
https://doi.org/10.1016/j.isci.2024.110039

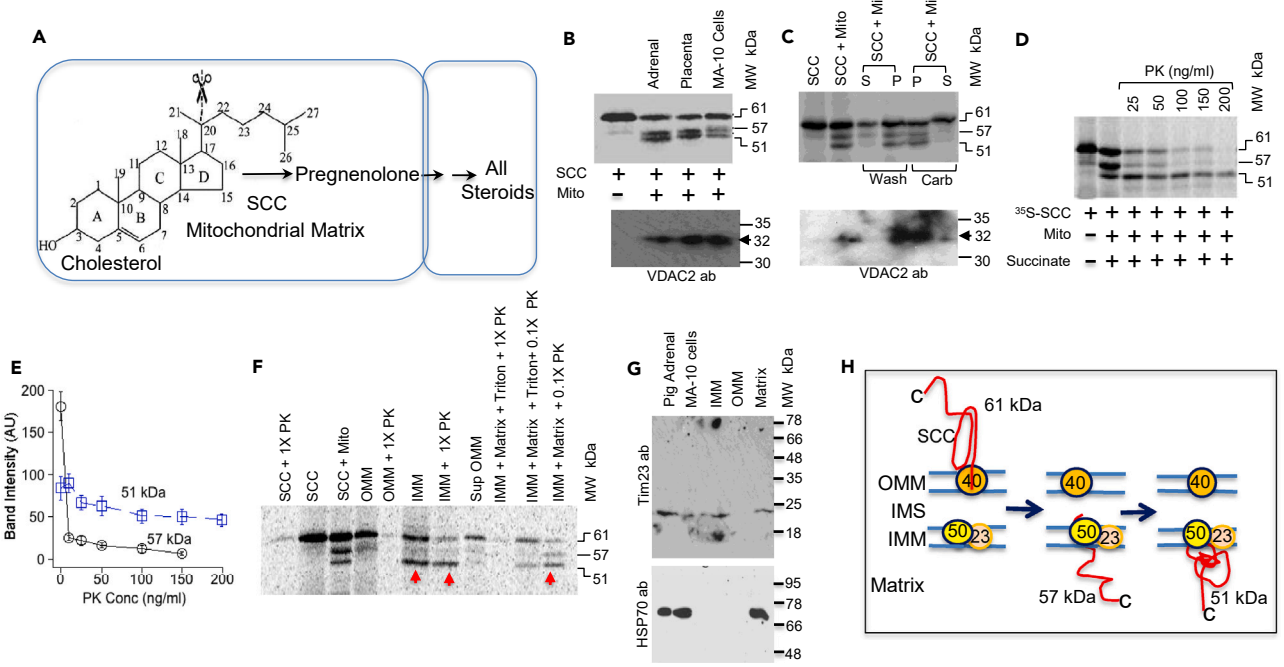

Figure 1. Partially unfolded and folded SCC association with the matrix side of the IMM

(A) Schematic presentation of cholesterol to pregnenolone catalysis by SCC.

(B) Top, mitochondrial import and processing of SCC. ^{35}S- cell free synthesized SCC was imported into the mitochondria isolated from pig adrenals, placenta, and MA-10 cells. The 61-kDa SCC was imported into 57- and 51-kDa proteins. Bottom, western blot of the mitochondria applied for import experiments with a VDAC2 antibody showing the presence of identical amounts of mitochondria applied to each reaction.

(C) Top, integration of imported SCC proteins. After import of ^{35}S-SCC with isolated mitochondria, the imported (P) fraction was separated from non-imported fraction (S) by washing followed by centrifugation. In some cases, following import the fractions were extracted with Na_2CO_3 at pH 11.5 followed by separation with a centrifugation. Bottom, western blot of the membrane shown in the top panel with a VDAC2 antibody.

(D) Incubation with varying concentrations of proteinase K (PK) following import of ^{35}S-SCC into the freshly isolated mitochondria for 30 min.

(E) Semiquantitative analysis of the integration of the 57-kDa (Solid line in black with round circle, ——○——) and 51-kDa (broken small solid lines in blue with square, –□- -) SCC and its protection from PK from (D). The Y axis is the band intensity in arbitrary phosphorimager units (AU), and X axis is PK concentration.

(F) Following mitochondrial import of ^{35}S-SCC, mitochondria were fractionated into OMM, IMM, and matrix fractions followed by incubation with 0.4% Triton X- and with two different concentrations of PK (500 ng/mL [1X] and 50 ng/mL [0.1X]).

(G) Western blot of the mitochondrial fractions with antibodies specific for the IMM resident, Tim23, (Top) and matrix resident, HSP70, (bottom).

(H) Schematic presentation showing SCC import into mitochondria and its association with the mitochondrial membrane first as a 57-kDa protein, which is then folded completely and remained integrated with the IMM facing the matrix. Data in (E) are presented as the mean ± S.E. of three independent experiments $p < 0.05$.

catalysis from pregnenolone to progesterone.[22] The first step of catalytic reaction is crucial, as cholesterol catalysis by SCC involves two successive monooxygenation reactions followed by the SCC-catalyzed C–C cleavage of 20R,22R-dihydroxycholesterol bond (Figure 1A). The bond cleavage is mediated by H-abstraction. The multiple steps involving electron transport chain are associated actively folded SCC availability, and a delay in active state formation results in reduced or no cholesterol catalysis.

The molecular mechanism underlying mitochondrial complex formation and electron transport for initiation and delay of steroid metabolic activity remains unclear. We have previously shown that SCC requires interaction with Tim50 mitochondrial translocase for its activity,[23] where electrostatic interaction requiring an enthalpy (ΔH) of −6.5 kCal/mole is necessary for catalyzing the cholesterol reaction in the matrix.[24] Here, we identified the steps associated with SCC folding to reach an activated state in the IMM. We report that formation of a molten globule, which lacks close packing of amino acid side chains that characterize the native state of a protein having more water molecules in the core,[19] is an intermediate step in the kinetic (and sometimes thermodynamic) pathway between native and unfolded states.[25,26] The molten globule can form in an orderly fashion occurring late in protein folding processes resulting activity[22] or can be a disordered fashion forming early folding intermediates resulting no activity.[27] Therefore, the transition state has the properties of a dry molten globule, that is, high free energy and low configurational entropy, being structurally similar to the native state.[28] By analyzing the intermediate protein folding steps, we show that a dry molten globule exits in the mitochondrial matrix of adrenal cells, which remains in a minimally active state with a limited network of interaction. The dry molten globule becomes active with the availability of additional hydrogen ions, forming a wet molten globule state activating the organellar proteostatic mechanism and trigging mitochondrial metabolism.

RESULTS

Imported intermediate SCC is folded to a mature state in the matrix

SCC is synthesized in free-floating ribosomes,[13] after which it translocates to mitochondria to initiate cholesterol catalysis. Under acute stimulation, SCC does not instantly catalyze cholesterol. We hypothesize that this delay is due to folding requirements for SCC following its mitochondrial import and prior to cholesterol catalysis.[29] We first determined ^{35}S-SCC import into the isolated metabolically active mitochondria of different steroidogenic tissues and cells (Figure S1). As shown in Figure 1B, full-length 61-kDa SCC is processed in mitochondria as 57- and 51-kDa protein fractions, suggesting that its two-step processing is identical in all tissues and cells (Figure 1B). Western blotting with an antibody specific for an OMM-associated protein, VDAC2, showed similar expression in each import reaction (Figure 1B, bottom panel), confirming uniform quantities of mitochondrial presence in all import experiments.

Interestingly, the imported 57- and 51-kDa SCC proteins were of similar intensity in all the tissues (Figure 1B), suggesting that until the already imported 51-kDa protein is disposed from the matrix, newly processing of the 57-kDa protein to 51 kDa does not occur, which is suggestive of a two-step process after the first cleavage and refolding step. To confirm this hypothesis, ^{35}S-SCC was imported into the freshly isolated mitochondria, and the imported fractions were first separated from the unimported by centrifugation followed by extraction with Na_2CO_3, which breaks protein-protein interactions but not lipid-protein interactions.[30] As shown in Figure 1C, full-length 61-kDa SCC is imported into the mitochondria into two smaller fragments of 57 kDa and 51 kDa. Following washing or carbonate extraction, both the fragments remained in the pellet, confirming membrane integration. Therefore, we concluded that SCC is processed into mitochondria in two-step membrane-integrated mechanism.

To understand the folding state of the SCC-imported fractions, we next evaluated specific mitochondrial membrane and compartmental integration with limited proteolysis, as the mitochondrial membrane transiently protects proteins from proteolysis, whereas unimported or partially imported proteins will be rapidly proteolyzed. As shown in Figure 1D, following ^{35}S-SCC import into isolated mitochondria, 57-kDa SCC was largely proteolyzed with a minimal concentration of 25 ng proteinase K (PK) without affecting the 51-kDa protein. The 51-kDa protein was resistant to proteolysis up to 150 ng PK (Figure 1D), indicating that the mitochondrial membrane shielded the 51-kDa protein from proteolysis. Quantitative analysis of the mitochondrial processing efficiency (Figure 1E) showed that the rapid proteolysis of the 57-kDa protein may be due to its unfolded state allowing PK access,[18,19] and resistance to proteolysis of the 51-kDa protein suggests a folded state.

We next determined mitochondrial-specific compartmental integration intensity of the imported fractions by isolating the OMM, IMM, and matrix following SCC import and proteolyzing with PK in presence and absence of a detergent (Triton X-100). As shown in Figure 1F, the integrated 51-kDa protein present in the matrix was resistant to PK, but not the matrix-associated 57-kDa protein. To confirm easy accessibility of the 57-kDa open state, we incubated the mitochondrial fractions with Triton X-100 and 10-fold difference in concentration of PK. Triton X-100 forms a micelle, where the micelle monomer enters the pores and is adsorbed on the internal surfaces with a monomer size of Triton X-100 resulting in an elliptical micelle facilitating easy access of PK. In the presence of Triton X-100, the IMM-associated 57-kDa protein was proteolyzed with lower concentrations of PK (Figure 1F). Although the 51-kDa SCC was resistant to proteolysis with higher concentration of PK, it was proteolyzed after inclusion of Triton X-100 (Figure 1F). Accuracy of the fraction separation was confirmed by western blotting for IMM-specific Tim23 (Figure 1G, top panel) and matrix-specific HSP70 antibodies independently (Figure 1G, bottom panel). Tim23 is an IMM-integrated protein present at the intermembrane space (IMS) side of the TIM23 complex, which mediates the translocation of transit peptide-containing proteins across the mitochondrial inner membrane.[4,31] Interestingly, SCC-associated independent mitochondrial fractions are not active (Figures S2A and S2B). In summary, following 61-kDa SCC import through the mitochondrial import channel, both the 57- and 51-kDa proteins were integrated with the IMM facing the matrix, with the 57-kDa protein less tightly folded, possibly due to a stable intermediate state (Figure 1H).

SCC moves from openness at the matrix to a closed state

We next hypothesized that the intermediate 57-kDa state is native-like but lacking close packing in the matrix. Therefore, we captured the 57-kDa SCC intermediate to understand its folding. We unfolded SCC with different concentrations of urea prior to import and assayed mitochondrial import kinetics. Urea indirectly promotes protein unfolding by altering water structure and dynamics, thereby diminishing the hydrophobic effect and facilitating the exposure of the hydrophobic core residues.[32] In the absence of urea, SCC was imported into 57- and 51-kDa proteins, and addition of 1.0 M urea reduced levels of the 51-kDa protein, which was completely absent with 2M urea (Figure 2A). Interestingly, processing from 61- to 57-kDa SCC was stopped with urea concentrations greater than 3M and resulted a SCC-urea covalently linked 61.6 kDa protein. Quantitative analysis showed that 51-kDa processing from the 57-kDa protein was stopped with increasing urea concentrations of 1M or more (Figure 2B). Urea eliminates ammonia by hydrogen transfer between the two amino groups of the peptide by a water molecule, resulting in the formation of a zwitterionic intermediate, H_3NCONH. The 57-kDa protein was stabilized by zwitterion in a state through extended hydrogen-bonding,[33] resulting a complete stable intermediate state in the matrix.

Dry molten globule has a limited network of interacting proteins

The 57-kDa protein is a stable intermediate in the mitochondria[34,35]; therefore, we determined its network of interaction with mitochondrial translocases. We first determined the localization of 57-kDa SCC at the cellular level. Incubation of 2M urea for 24 h did not alter MA-10 cell structure through light microscopy compared to the untreated cells (Figure 2C). TEM analysis of mitochondrial structure with 2M urea showed

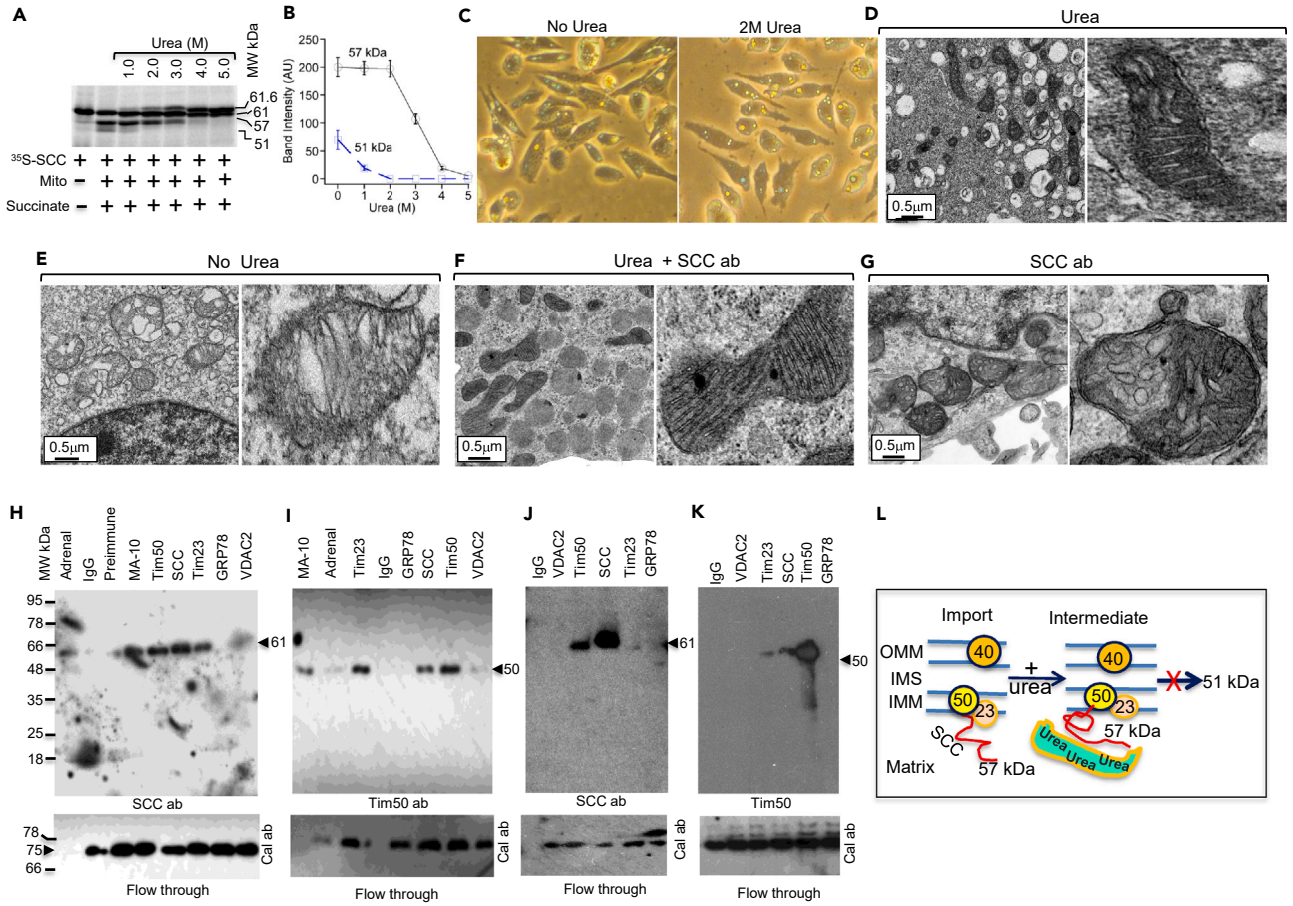

Figure 2. Intermediate state is stable with limited interaction with the translocase network

(A) Import of ^{35}S-SCC into the freshly isolated mitochondria for 1 h incubated with the indicated concentrations of urea prepared with the import buffer pH 7.4.

(B) Semiquantitative analysis of the intensity of SCC imported 57-kDa (Solid line in black with round circle, ——○——) and 51-kDa (Broken small solid lines in blue with square, - -□- -) proteins into the mitochondria. The Y axis is the band intensity in arbitrary units (AU), and X axis is the urea concentrations. Data in (B) are presented as the mean ± S.E. of three independent experiments and $p < 0.05$.

(C) Light microscopic visualization of the MA-10 cells with (left) and without (right) 2M urea for 24 h.

(D and E) Direct visualization of the change in mitochondrial structure with (D) and without (E) urea. The right (D and E) are the enlarged magnification of a mitochondrion from the left. The scale bar for (D and E) is 0.5 nm.

(F and G) Localization of SCC by nanogold labeling following with (F) or without (G) urea incubation using an SCC antibody. The nanogold particle size 15 nm with the scale bar is 0.5 nm. The right panel is the enlargement of a mitochondrion from the left.

(H–K) CoIP analysis in MA-10 cells with (J and K) or without (H and I) urea for 24 h with the indicated antibodies followed by Western blotting with SCC (H and J) and Tim50 (I and K) antibodies independently. Bottom, flowthrough western blot with a calnexin antibody.

(L) Schematic presentation showing import of the 57-kDa protein into mitochondria that remains fully protected as an intermediate by the zwitterionic urea molecule.

no difference from the untreated cells (Figures 2D and 2E), which was further shown in enlarged views of a mitochondrion in the right panels of Figure 2D and 2E. The zwitterionic urea intermediate molecule, H_3NCONH, did not affect the cellular architecture possibly due to the solvation effect blocking the SCC backbone.[36] Next, nanogold labeling with an SCC antibody showed localization in the mitochondrial matrix both in the presence (Figure 2F) and absence (Figure 2G) of urea, confirming that integration of the SCC was unchanged in cells exposed to 2M urea (Figure 2F, right panel). Due to the lack of hydrogen ions with urea in the matrix, it is most likely that SCC is in the 57-kDa state, a stably folded state.

SCC is a member of ETC complex II,[24] and requires the mitochondrial translocase, Tim50, for metabolic activity.[23] To determine the urea-induced SCC protein (57-kDa) network of interaction, we incubated steroidogenic MA-10 cells with 2M urea for 24 h, isolated mitochondria, and examined interactions with Tim50 by coIP experiments. In this analysis using specific antibodies, we first isolated mitochondrial Tim50, VDAC2, SCC, and Tim23 as well as ER-specific GRP78 antibody as a negative control followed by staining with SCC and Tim50 antibodies independently (Figures 2H–2K). Flow through was stained with calnexin antibody (Figures 2H–2K, bottom panels). As expected, Tim50 and SCC interaction was unchanged in the presence of urea, but no interaction with VDAC2 and GRP78 was observed (Figures 2J and

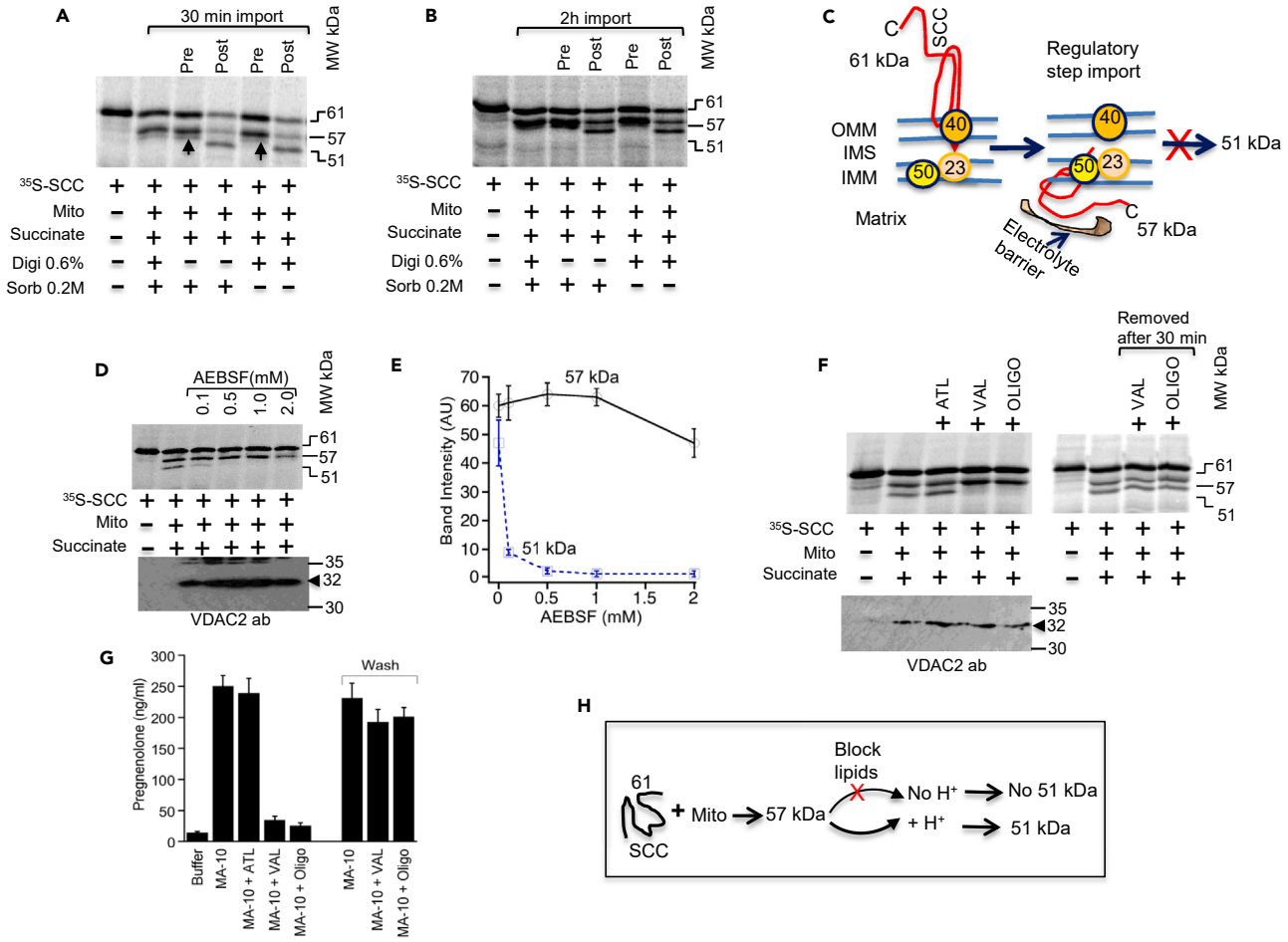

Figure 3. Hydrogen ions shield processing at the intermediate state

(A and B) Import of ^{35}S-SCC for 30 min (A) and 2 h (B) in the presence of sorbitol and digitonin together or independently before or after equilibrating freshly isolated mitochondria from MA-10 cells.

(C) Schematic presentation of arresting 57-kDa intermediate state at the matrix with the osmolyte barrier for electrolytes.

(D) Left, Import of ^{35}S-SCC for 2 h in the presence of various concentrations of AEBSF. Bottom, western blotting with a VDAC2 antibody.

(E) Semiquantitative analysis of the processing of 57- and 51-kDa SCC in the presence of different concentrations of AEBSF from the top of (D).

(F) Top left, Mitochondrial import ^{35}S-labeled SCC for 1 h in the presence of atractoloside (ATL), oligomycin (Oligo), and valinomycin (Val) for 1 h. Top right, After incubation for 1 h, the inhibitors were removed by dialysis against import buffer followed by washing and centrifugation, and imported for 1 h under identical conditions. Bottom left, western blotting analysis a VDAC2 antibody.

(G) SCC activity (pregnenolone synthesis) in the presence of inhibitors and after removal of inhibitors in (F).

(H) Schematic cartoon showing the requirement two hydrogen ions for the processing of the intermediate state to an active folded state. Data presented in (E and G) as the mean ± S.E. of three independent experiments and $p < 0.05$.

2K). Tim23, which is part of the TIM23 complex containing the Tim50 translocase at the IMM, showed a minor interaction. Thus, although the individual expression of SCC or Tim50 was not reduced with urea, the network of interaction was reduced. Therefore, the energy (-ΔH -6.5 kCal/mole) required to reach the transition state hydrolysis preserved the 57-kDa folding state by maintaining an energy balance with the lack of hydrogens.[24,37] Therefore, the intermediate 57-kDa folding is a dry molten globule[35] (Figure 2L).

Salt bridges stabilizes intermediate 57-kDa folding

Protein stability depends on the interactions of the amino acid side chains and secondary structure with the cellular environment through the hydrogen bonds and salt bridges, contributing to the overall stability.[38] We hypothesize that SCC goes through an additional folding process to produce the active 51-kDa state to catalyze the cleavage of C20-C22 cholesterol bond. To determine whether 57-kDa SCC is a stable state that requires additional time to be in an active folded state, we blocked the availability of hydrogen ions by importing SCC in the presence of an osmolyte. Osmolytes, like sorbitol, are small molecules that are used by cells to counter osmotic stress,[39] because the polyol and sugar osmolytes preferentially exclude hydrogen ions from the protein surface. Following import of the 61-kDa protein for 30 min (Figure 3A) or

2 h (Figure 3B) in the presence of sorbitol or digitonin alone or together, only 57-kDa protein was observed, suggesting that protein folding was induced by sorbitol. The presence of osmolytes perturbed the intramolecular hydrogen bonds; therefore, the presence of sorbitol decreased the site-specific exchange rates, suggesting that the local conformational opening is less frequently consistent with the hydrogen bond strengthening effect (Figure 3C).[38,40]

We next modified serine residues of SCC amino acids without any change in amino acids by 4-benzenesulfonyl (2-aminoethyl) fluoride hydrochloride (AEBSF) and determined its processing through the mitochondrial membrane by import assays. AEBSF interacts with the hydroxyl groups of serine residue to form a highly stable sulfonyl enzyme.[41] After addition of 0.1 μM AEBSF during mitochondrial import, only 57-kDa SCC was detected (Figure 3D). A 50-fold increase in AEBEF showed unchanged processing of the 57-kDa protein suggesting that the intermediate state was shielded with no available hydrogens to exchange (Figure 3E), thus stabilizing the intermediate folding state.

We next asked the driving force maintaining the 57-kDa intermediate state by determining the impact of valinomycin (Val) and oligomycin (Oligo) on mitochondrial import (Figure 3F). SCC import and processing is ATP-independent,[24] so addition of an ADP transport inhibitor, atractoloside (ATL), was ineffective (Figure 3F). Oligomycin binds to the ATP synthase subunit consisting of two helices spanning into the IMM, thereby preventing protons from passing back into the mitochondria and stopping the proton pumps as the gradients become too high to remain functional. Therefore, imported 57-kDa SCC is blocked access to hydrogen.[23] To confirm that the 57-kDa requires additional hydrogens to be processed into the 51 kDa protein, SCC mitochondrial import was evaluated in the presence of valinomycin, a resembling cyclic peptide. Valinomycin is uncharged with no ionizable groups that act directly on phospholipid membranes to increase their cation permeability. As seen in Figures 3F and S3, 51-kDa protein was absent in the presence of oligomycin and valinomycin but was restored when valinomycin or oligomycin were removed by washing (Figure 3F, right panel), resulting in pregnenolone synthesis (Figure 3G, right panel). Therefore, additional hydrogen ions are required for conversion of 57- to 51-kDa SCC (Figure 3H) suggesting the formation of a folded metabolically active protein from a dry molten globule state to a wet molten globule state.

C-terminus dictates SCC folding

SCC goes through multiple folding states where it might require low energy depending on the angles, distances, and prevalence of the trans peptide bonds and side chain rotamers.[42] We hypothesized that segment(s) of SCC dictates its overall folding.[43] We determined the minimum SCC amino acids necessary for mitochondrial import creating SCC fusions by gradually deleting the C-terminal amino acids followed by fusion with full-length DHFR at the C-terminus (Figure 4A). DHFR is a cytoplasmic resident 186 amino acid protein with a parallel β-sheet structure and participates in longer-range contacts for the development and stability of the tertiary structure.[44,45] Import experiments showed 57- and 51-kDa protein with the wild-type SCC (Figure 4B); however, the 83-kDa SCC(1–511)-DHFR-C fusion generated only a 73-kDa protein (Figure 4C), suggesting direct conversion from full-length to final folded state having no intermediate folding. Similar results were observed with further C-terminal deleted fusions (Figure 4D and 4E), suggesting that the N-terminus is independent of the C-terminal passenger protein folding.[8,9]

We next hypothesized that the SCC C-terminus stabilizes its overall folding. The conformational flexibility of the C-terminus enables induced fit interactions through one or more C-terminal minimotifs. Therefore, we next added an extra ten amino acids of DHFR to the C-terminus of SCC (Figure 4F), generating a fusion protein of SCC-DHFR of 531 amino acids, which on mitochondrial import shows 62- and 56-kD proteins, a cleavage pattern similar to wild-type SCC (Figures 4H and S4). Incubation with PK showed almost no resistance of the 57-kDa protein to PK (Figure 4H), as compared to the wild-type SCC (Figure 4G). Similar results were observed with the additional fusions (Figure S4). The motif at the C-terminus is similar to an α-helix pattern[46] with a 1.3-fold preference for α-helices in the C-terminus over the N-terminus.[47] Therefore, addition of ten amino acids changed the C-terminus local contacts from an α-helix to β-turn or coiled-coiled secondary structure,[46] resulting an open conformation accessible (Figure 4I).

SCC C-terminus is independently folded for stability

Minimotifs are short, linear motifs with shorter functional components of proteins necessary and sufficient for trafficking of proteins to specific subcellular localizations.[48,49] We hypothesized that deletion of amino acids from the C-terminus having parallel β-sheets structure participate in longer-range contacts. To evaluate this, we gradually deleted amino acids from the C-terminus, generating C-10, C-20, C-50, and C-100 SCC proteins (Figure 5A) that were imported into isolated mitochondria. Whereas wild-type SCC generated 57- and 51-kDa proteins with the 57-kDa intermediate resistant to 50 ng/mL PK (Figure 5B); however, the other C-terminal deletional mutants did not generate any intermediate protein (Figures 5C and S5). Quantitative analysis of the 57- and 51-kDa protection is shown in Figures 5D and 5E. Absence of the intermediate protein suggests that the C-terminus played an intermediate folding step, suggesting that the C-terminal sequence builds minimotifs and plays an active role in SCC folding.

We next determined the activity of these C-terminal deletional mutants by transfecting nonsteroidogenic COS-1 cells. To our surprise, deletion of only ten amino acids reduced activity, generating 34.3 ± 3.9 ng/mL pregnenolone as compared to 82 ± 7.2 ng/mL with the wild-type SCC. The activity of all other mutants was similar to the empty vector control (Figure 5F). The SCC 3-dimentional structure shows that both hydroxyls are close to the heme iron but without direct interactions. As the hydroxyl group needs to be close to the heme iron for initiating electron transfer, therefore, positioning for the substrate is unique, leaving limited space for oxygen binding to the reduced heme iron and increasing the possibility for cholesterol accommodation due to the flexibility of the SCC side chain.[29] In the absence of C-terminal sidechain amino acids, hydrogen ions could not be added, and minimotifs were not formed (Figure 5G) because solvation of the peptide NH

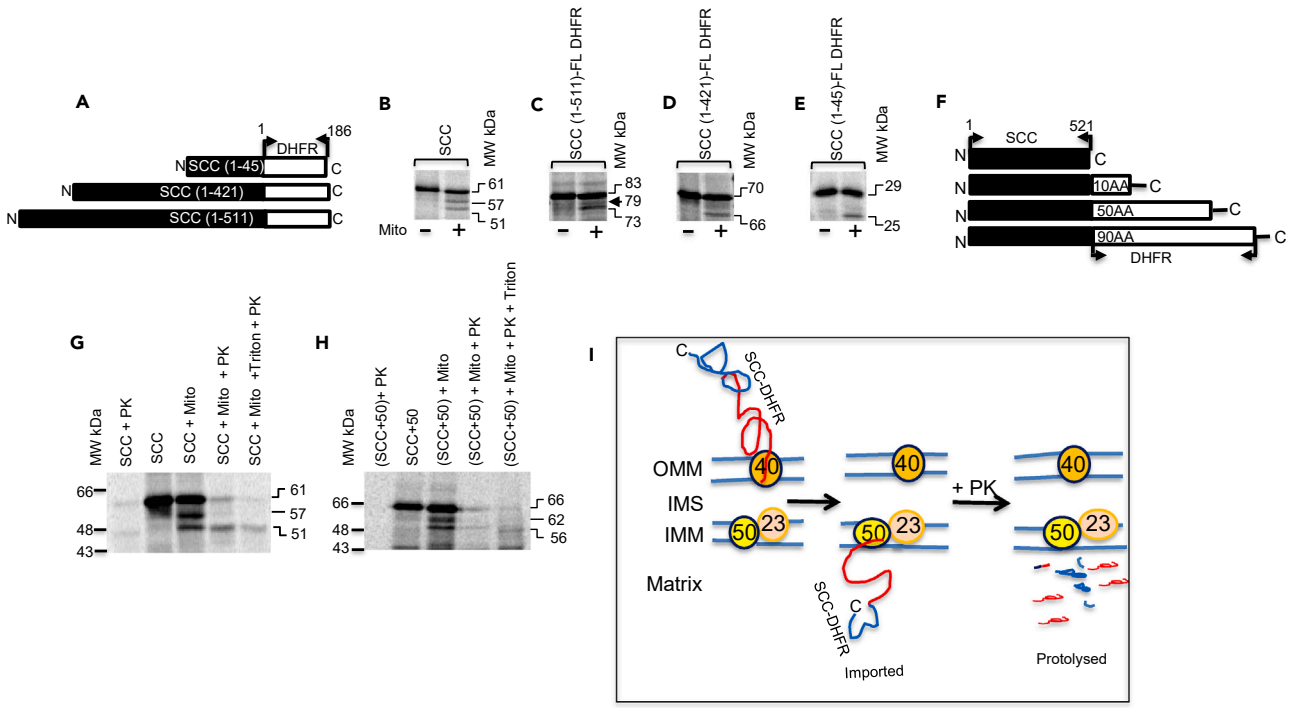

Figure 4. Role of N- and C-termini of SCC in mitochondrial import

(A) Schematic presentation of C-terminal deleted SCC fusions with DHFR.

(B–E) Import of the ^{35}S-SCC and different SCC-DHFR fusions from (A) into the isolated mitochondria for 1 h.

(F) The C-terminus is the regulatory region for overall SCC folding. Schematic presentation of different fusion constructs with the addition of amino acids from DHFR with the C-terminal region of SCC.

(G and H) Integration of SCC (G) and N-(1-521SCC)+(1–50 DHFR)-C fusion (H) following mitochondrial import. Following mitochondrial import of ^{35}S- SCC (G) or SCC fusion (H), proteins were treated with and without PK in the presence and absence of 0.5% Triton X-100.

(I) Schematic presentation showing that the import of C-terminal SCC fusion following its import into the mitochondria remained associated with the IMM facing the matrix, which is easily proteolyzed with minimal concentrations of PK.

and CO groups arise from neighboring residue effects, with sidechain shielding of peptide groups.[50] In summary, it appears the C-terminus independently folds, resulting in a final folding of the protein.

DISCUSSION

Cholesterol is the only substrate in the mitochondrial matrix, where its side chain is cleaved by SCC releasing six amino acids in solution. SCC enzymatic activity is maintained by accurate folding, which is required for recognition and guidance from the IMM to its active site. The SCC crystal structure suggests that the F–G loop and the A′ helix comprise the IMM hydrophobic surface that interacts with the membrane.[51] The 3β-hydroxyl of cholesterol does not interact with SCC residues but binds to two water molecules, which are part of a hydrogen-bonded network formed by additional water molecules and polar residues.[29] Tim50 is a central receptor of mitochondrial complex and recognizes precursor proteins in the IMS. Tim50 also interacts with the IMS domain of the channel forming subunit, Tim23, an interaction that is essential for protein import and translocation across the mitochondrial inner membrane. Tim50 either by depletion of the protein from the TIM23 complex or addition of anti-Tim50 antibodies block the protein translocation across the inner membrane[52] and reduces activity steroidogenic activity in adrenal and gonadal cells.[9,23] Maintenance of the Tim50 mitochondrial network is crucial for metabolic activity because in the absence of hydrogen bonding, SCC is easily proteolyzed suggesting easy access to the protein core. Lack of hydrogen ions also led to the formation of a dry molten globule.

The minimum N-terminal amino acids of SCC fused with complete cytoplasmic DHFR fusion (Figures 4A and 4E) bring the SCC-DHFR to the matrix side of IMM, but fusion of the N-terminus with the cytoplasmic sequence prevented mitochondrial import.[53] SCC N-terminal fusion with other mitochondrial resident proteins did not compete with each other during mitochondrial import, suggesting that the SCC N-terminal sequence is unique.[16] Oligomycin with its 26-numbered lactone core fused to a spiroketal moiety with a hydroxypropyl side chain stereoselectively controlled hydrogen bonding of dienophile with the side-chain isopropanol moiety and secondary orbital interactions.[54] During SCC import, oligomycin stabilized the folding state of the 57-kDa protein but not the 51-kDa protein (Figures 3D, 3E, and S3). Therefore, the rate limiting step in SCC activation is the release of the intermediate, 57-kDa, protein which forms a dry molten globule. Once two hydrogen ions are available, SCC folding changes from the partially active state to the fully active folded state.

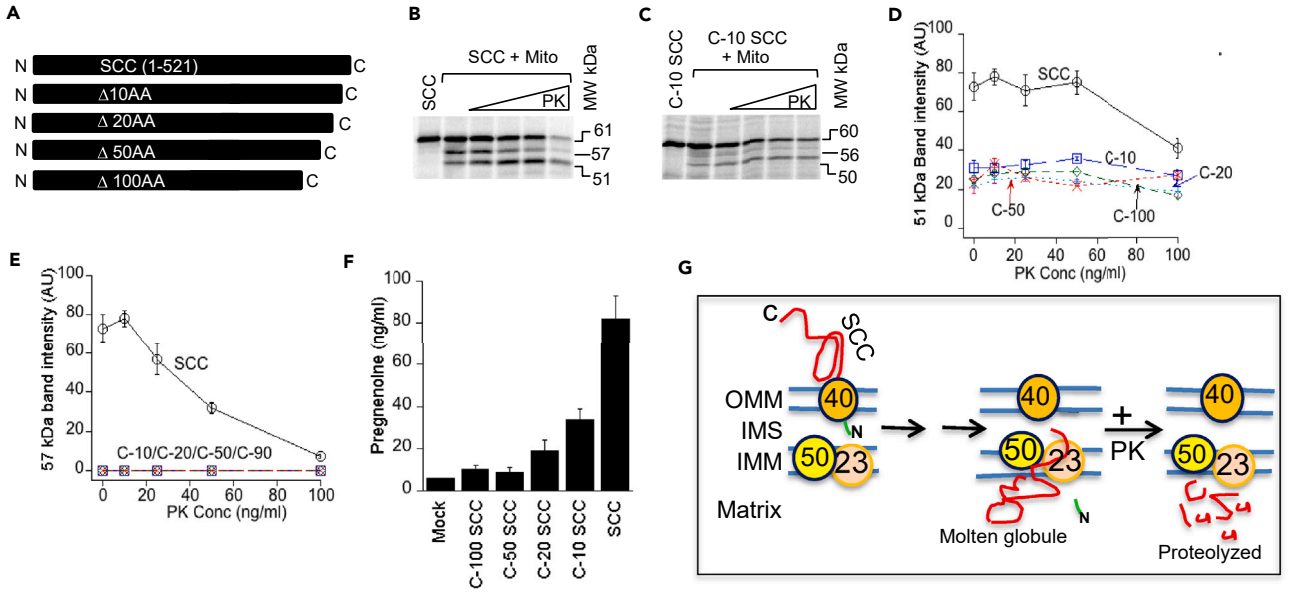

Figure 5. Minimotifs are generated from the C-terminus

(A) Design of the different C-terminal SCC deletional mutants.

(B and C) Import of the ^{35}S-SCC and the deletional constructs from the (A) for 1 h in the presence of varying concentrations of PK.

(D and E) Intensity of protection of the 51-kDa (D) and 57-kDa (E) imported proteins in the presence of varying concentration of PK and its relation to the length of the C-terminal amino acids. The X axis is the different concentrations of PK, while Y axis represents represent the intensity of protection.

(F) SCC activity (pregnenolone) co-transfected with the truncated C-terminal deletional mutants with ferredoxin, ferredoxin reductase, and StAR cDNA in COS-1 cells. The X axis is the wild-type SCC and SCC mutants, while Y axis represents the amounts of pregnenolone synthesized after 42 h of transfection. Data in (D–F) are presented as the mean ± S.E. of three independent experiments and $p < 0.05$.

(G) Schematic presentation of the formation of unstable folding in the absence of far C-terminal amino acids, resulting a state easily susceptible to proteolysis.

Protein folding is generally a rapid process; however, SCC requires three successive steps for complete conformational change to its active state.[55] These conformational changes are associated with the stabilization of enthalpy (ΔH) −5.6 kCal/mole.[24] SCC first requires stabilization followed by two folding events prior to activation. The SCC intermediate state is stabilized due to the lack of hydrogen ions, which finally determines whether the 57-kDa protein will be converted to a mature, folded state.

Steroid hormone biosynthesis begins with the conversion of cholesterol to pregnenolone in the mitochondrial matrix side, involving two successive monooxygenation events catalyzed by SCC and cleavage of 20R,22R-dihydroxycholesterol. The process involves extensive bond breakage reactions requiring energetic minimization, where the C20–C22 bond cleavage is mediated by H-abstraction from C20-OH. Therefore, unfolding of the 57-kDa intermediate is not influenced by the cellular chaperones, but is dependent on the environment as well as its amino acid sequence. Based on these data, we have concluded that SCC is in a molten globule state immediately after import, which promotes activity. The intermediates comprised partially folded forms of individual domains or of the entire protein. Molten globules can be viewed as highly dynamic, collapsed, compact polypeptide chains maintained by hydrophobic interactions that promote helical conformations but that lack fixed, specific long-range interactions; thus, biological activity is highly questionable at the molten globule state. This folding state likely occurs in eukaryotic mitochondrial proteins as the membrane insertion pathway is fairly conserved[56] supporting that the dry molten globule is inherently conserved during steroid metabolism.

In conclusion, most proteins fold into a unique, thermodynamically stable, and three-dimensional conformation *in vitro*. Protein folding *in vivo* is extremely intricate because the conformational changes, including folding, misfolding, and aggregation, can be influenced by the cellular environment and required much longer time to be folded (up to minutes).[57] The physical-chemical principles of protein folding processes are difficult to fully understand as multiple factors in addition to chaperones are involved in the accurate folding process, where some proteins are active in an intermediate state.[8,18,58] Theoretical studies have shown that the free energy landscapes for protein folding are most often biased like a funnel toward the structurally well-defined native state. SCC folding inside the cell involves multiple parameters, including molten globules that represent a transition state to final, active state with the addition of electrons. The intermediate *in vivo* step is a dry molten globule folded state with a minimum network of interaction that is activated with the additional hydrogen ions from water molecules, leading to catalytic activation of the conversion of cholesterol to pregnenolone.

Limitations of the study

The current study was limited using the urea concentration 2M and diluted to 1M for all experiments and could not be continued because of the increase in cell death. The urea concentration was not determined before and after incubation at 37°C as the amino acids and serum used

in growing cells prevented for accurate urea concentration. Similarly, we could not directly use the live cells to determine the SCC folding inside the cells. The protein synthesized through cell-free transcription translation system also inhibited an accurate amount of protein synthesized and was limited to an indirect measurement by western blotting and radiolabeling.

STAR★METHODS

Detailed methods are provided in the online version of this paper and include the following:

- KEY RESOURCES TABLE
- RESOURCE AVAILABILITY
  - Lead contact
  - Materials availability
  - Data and code availability
- EXPERIMENTAL MODEL AND SUBJECT DETAILS
  - Plasmid construction, cell culture, mitochondria isolation and transfection
- METHOD DETAILS
  - Isolation of mitochondria and activity
  - *In vitro* synthesis and processing of the precursor protein with different mitochondrial fractions
  - Urea unfolding
  - Western blot analysis
  - Co-immunoprecipitation (co-IP) analysis
  - Transmission electron microscopy (TEM)
- QUANTIFICATION AND STATISTICAL ANALYSIS
  - Statistical analysis

SUPPLEMENTAL INFORMATION

Supplemental information can be found online at https://doi.org/10.1016/j.isci.2024.110039.

ACKNOWLEDGMENTS

H.S.B. was previously supported by grants from the NIH (RO1 HD057876) during the progress of this work and Seed Grant from Mercer University. The authors are thankful to Drs. Walter L Miller from UCSF for the SCC, Ferredoxin and Ferredoxin reductase cDNA, Bon-chu Chung for the SCC antibody, and Brendan Marshall from Augusta State University (Medical College of Georgia) for the TEM experiments. H.S.B. is also thankful to all the current and previous members of the lab in Hoskins Research Laboratory, especially to Mr. Curtis Lanier. H.S.B. is also thankful to Drs. Wei-Hsiung Yang, Mahuya Bose, Zhi-Qing Zhao, and Ms. Meenakshi Bose for critically reading the manuscript.

AUTHOR CONTRIBUTIONS

H.S.B. hypothesized, designed all the experiments, analyzed data, and wrote the paper.

DECLARATION OF INTERESTS

The authors declare no competing interest.

Received: December 1, 2023
Revised: February 18, 2024
Accepted: May 16, 2024
Published: May 21, 2024

REFERENCES

1. Russell, O.M., Gorman, G.S., Lightowlers, R.N., and Turnbull, D.M. (2020). Mitochondrial diseases: hope for the future. Cell *181*, 168–188.
2. Bhargava, A., Arnold, A.P., Bangasser, D.A., Denton, K.M., Gupta, A., Hilliard Krause, L.M., Mayer, E.A., McCarthy, M., Miller, W.L., Raznahan, A., and Verma, R. (2021). Considering sex as a biological variable in basic and clinical studies: an endocrine society scientific statement. Endo Rev. *42*, 219–258.
3. Coyne, L.P., Wang, X., Song, J., de Jong, E., Schneider, K., Massa, P.T., Middleton, F.A., Becker, T., and Chen, X.J. (2023). Mitochondrial protein import clogging as a mechanism of disease. Elife *12*, e84330.
4. Pfanner, N., Warscheid, B., and Wiedemann, N. (2019). Mitochondrial proteins: from biogenesis to functional networks. Nat. Rev. Mol. Cell Biol. *20*, 267–284.
5. Chacinska, A., Koehler, C.M., Milenkovic, D., Lithgow, T., and Pfanner, N. (2009). Importing mitochondrial proteins: machineries and mechanisms. Cell *138*, 628–644.
6. Neupert, W., and Herrmann, J.M. (2007). Translocation of proteins into mitochondria. Annu. Rev. Biochem. *76*, 723–749.
7. Clark, B.J., Wells, J., King, S.R., and Stocco, D.M. (1994). The purification, cloning and expression of a novel luteinizing hormone-induced mitochondrial protein in MA-10 mouse Leydig tumor cells. Characterization of the steroidogenic acute regulatory protein (StAR). J. Biol. Chem. *269*, 28314–28322.

8. Bose, H.S., Bose, M., and Whittal, R.M. (2023). Tom40 in cholesterol transport. iScience *26*, 106386.
9. Pawlak, K.J., Prasad, M., Thomas, J.L., Whittal, R.M., and Bose, H.S. (2011). Inner mitochondrial translocase Tim50 interacts with 3β-hydroxysteroid dehydrogenase type-2 to regulate adrenal and gonadal steroidogenesis. J. Biol. Chem. *286*, 39130–39140.
10. Bose, H.S., Sugawara, T., Strauss, J.F., III, and Miller, W.L.; International Congenital Lipoid Adrenal Hyperplasia Consortium (1996). The pathophysiology and genetics of congenital lipoid adrenal hyperplasia. N. Engl. J. Med. *335*, 1870–1878.
11. Kaur, J., Rice, A.M., O'Conner, E., Piya, A., Buckler, B., and Bose, H.S. (2016). Novel SCC mutation in a patient of Mexican descent with sex reversal, salt-losing crisis and adrenal failure. Endocrinol Diabetes Metab. *2016*, 16-0059.
12. Penning, T.M., Wangtrakuldee, P., and Auchus, R.J. (2019). Structural and functional biology of aldo-keto reductase steroid-transforming enzymes. Endocr. Rev. *40*, 447–475.
13. Miller, W.L., and Auchus, R.J. (2011). The molecular biology, biochemistry, and physiology of human steroidogenesis and its disorders. Endocr. Rev. *32*, 81–151.
14. Miller, W.L. (2021). Steroidogenic electron-transfer factors and their diseases. Ann. Pediatr. Endocrinol. Metab. *26*, 138–148.
15. Miller, W.L., and Bose, H.S. (2011). Early steps in steroidogenesis: intracellular cholesterol trafficking. J. Lipid Res. *52*, 2111–2135.
16. Rajapaksha, M., Kaur, J., Bose, M., Whittal, R.M., and Bose, H.S. (2013). Cholesterol-mediated conformational changes in the steroidogenic acute regulatory protein are essential for steroidogenesis. Biochemistry *52*, 7242–7253.
17. Cettolin, E., Dalton, P.S., Kop, W.J., and Zhang, W. (2020). Cortisol meets GARP: the effect of stress on economic rationality. Exp. Econ. *23*, 554–574.
18. Bose, H.S., Whittal, R.M., Baldwin, M.A., and Miller, W.L. (1999). The active form of the steroidogenic acute regulatory protein, StAR, appears to be a molten globule. Proc. Natl. Acad. Sci. USA *96*, 7250–7255.
19. Privalov, P.L. (1996). Intermediate states in protein folding. J. Mol. Biol. *258*, 707–725.
20. Bose, H.S., Whittal, R.M., Huang, M.C., Baldwin, M.A., and Miller, W.L. (2000). N-218 MLN64, a protein with StAR-like steroidogenic activity is folded and cleaved similarly to StAR. Biochemistry *39*, 11722–11731.
21. Tuckey, R.C., Bose, H.S., Czerwionka, I., and Miller, W.L. (2004). Molten globule structure and steroidogenic activity of N-218 MLN64 in human placental mitochondria. Endocrinology *145*, 1700–1707.
22. Prasad, M., Thomas, J.L., Whittal, R.M., and Bose, H.S. (2012). Mitochondrial 3β-hydroxysteroid dehydrogenase enzyme activity requires reversible pH-dependent conformational change at the intermembrane space. J. Biol. Chem. *287*, 9534–9546.
23. Bose, H.S., Gebrail, F., Marshall, B., Perry, E.W., and Whittal, R.M. (2019). Inner mitochondrial translocase Tim 50 is central in adrenal and testicular steroid synthesis. Mol. Cell Biol. *39*, e00484-18. https://doi.org/10.1128/MCB.00484-00418.
24. Bose, H.S., Marshall, B., Debnath, D.K., Perry, E.W., and Whittal, R.M. (2020). Electron Transport Chain Complex II Regulates Steroid Metabolism. iScience *23*, 101295. https://doi.org/10.1016/j.isci.2020.101295.
25. Regan, L. (2003). Molten globules move into action. Proc. Natl. Acad. Sci. USA *100*, 3553–3554.
26. Judy, E., and Kishore, N. (2019). A look back at the molten globule state of proteins: thermodynamic aspects. Biophys. Rev. *11*, 365–375.
27. Redfield, C., Smith, R.A., and Dobson, C.M. (1994). Structural characterization of a highly–ordered 'molten globule' at low pH. Nat. Struct. Biol. *1*, 23–29.
28. Rico-Pasto, M., Zaltron, A., Davis, S.J., Frutos, S., and Ritort, F. (2022). Molten globule–like transition state of protein barnase measured with calorimetric force spectroscopy. Proc. Natl. Acad. Sci. USA *119*, e2112382119.
29. Strushkevich, N., MacKenzie, F., Cherkesova, T., Grabovec, I., Usanov, S., and Park, H.W. (2011). Structural basis for pregnenolone biosynthesis by the mitochondrial monooxygenase system. Proc. Natl. Acad. Sci. USA *108*, 10139–10143.
30. Li, J.M., and Shore, G.C. (1992). Reversal of the orientation of an integral protein of the mitochondrial outer membrane. Science *256*, 1815–1817.
31. Gomkale, R., Linden, A., Neumann, P., Schendzielorz, A.B., Stoldt, S., Dybkov, O., Kilisch, M., Schulz, C., Cruz-Zaragoza, L.D., Schwappach, B., et al. (2021). Mapping protein interactions in the active TOM-TIM23 supercomplex. Nat. Commun. *12*, 5715.
32. Bennion, B.J., and Daggett, V. (2003). The molecular basis for the chemical denaturation of proteins by urea. Proc. Natl. Acad. Sci. USA *100*, 5142–5147.
33. Zhang, Z., Dmitrieva, N.I., Park, J.-H., Levine, R.L., and Burg, M.B. (2004). High urea and NaCl carbonylate proteins in renal cells in culture and in vivo, and high urea causes 8-oxoguanine lesions in their DNA. Proc. Natl. Acad. Sci. USA *101*, 9491–9496.
34. Baldwin, R.L., Frieden, C., and Rose, G.D. (2010). Dry molten globule intermediates and the mechanism of protein unfolding. Proteins *78*, 2725–2737.
35. Jha, S.K., and Udgaonkar, J.B. (2009). Direct evidence for a dry molten globule intermediate during the unfolding of a small protein. Proc. Natl. Acad. Sci. USA *106*, 12289–12294.
36. Candotti, M., Esteban-Martín, S., Salvatella, X., and Orozco, M. (2013). Toward an atomistic description of the urea-denatured state of proteins. Proc. Natl. Acad. Sci. USA *110*, 5933–5938.
37. Alexandrova, A.N., and Jorgensen, W.L. (2007). Why urea eliminates ammonia rather than hydrolyzes in aqueous solution. J. Phys. Chem. B *111*, 720–730.
38. Chen, S., Itoh, Y., Masuda, T., Shimizu, S., Zhao, J., Ma, J., Nakamura, S., Okuro, K., Noguchi, H., Uosaki, K., and Aida, T. (2015). Subnanoscale hydrophobic modulationof salt bridges in aqueous media. Science *348*, 555–559.
39. Rani, A., and Venkatesu, P. (2018). Changing relations between proteins and osmolytes: a choice of nature. Phys. Chem. Chem. Phys. *20*, 20315–20333.
40. Li, J., Chen, J., An, L., Yuan, X., and Yao, L. (2020). Polyol and sugar osmolytes can shorten protein hydrogen bonds to modulate function. Commun. Biol. *3*, 528.
41. Powers, J.C., Asgian, J.L., Ekici, Ö.D., and James, K.E. (2002). Irreversible inhibitors of serine, cysteine, and threonine proteases. Chem. Rev. *102*, 4639–4750.
42. Butterfoss, G.L., and Hermans, J. (2003). Boltzmann-type distribution of side-chain conformation in proteins. Protein Sci. *12*, 2719–2731.
43. Bose, H.S., Whittal, R.W., Debnath, D., and Bose, M. (2009). Steroidogenic acute regulatory protein has a more open conformation than the independently folded domains. Biochemistry *49*, 11630–11639.
44. Horst, R., Fenton, W.A., Englander, S.W., Wüthrich, K., and Horwich, A.L. (2007). Folding trajectories of human dihydrofolate reductase inside the GroEL–GroES chaperonin cavity and free in solution. Proc Natl Acad Sci *104*, 20788–20792.
45. Bhabha, G., Ekiert, D.C., Jennewein, M., Zmasek, C.M., Tuttle, L.M., Kroon, G., Dyson, H.J., Godzik, A., Wilson, I.A., and Wright, P.E. (2013). Divergent evolution of protein conformational dynamics in dihydrofolate reductase. Nat. Struct. Mol. Biol. *20*, 1243–1249.
46. Laio, A., and Micheletti, C. (2006). Are structural biases at protein termini a signature of vectorial folding? Proteins *62*, 17–23.
47. Krishna, M.M.G., and Englander, S.W. (2005). The N-terminal to C-terminal motif in protein folding and function. Proc. Natl. Acad. Sci. USA *102*, 1053–1058.
48. Balla, S., Thapar, V., Verma, S., Luong, T., Faghri, T., Huang, C.-H., Rajasekaran, S., del Campo, J.J., Shinn, J.H., Mohler, W.A., et al. (2006). Minimotif Miner: a tool for investigating protein function. Nat. Methods *3*, 175–177.
49. Fortelny, N., Yang, S., Pavlidis, P., Lange, P.F., and Overall, C.M. (2015). Proteome TopFIND 3.0 with TopFINDer and PathFINDer: database and analysis tools for the association of protein termini to pre- and post-translational events. Nucleic Acids Res. *43*, D290–D297.
50. Avbelj, F., and Baldwin, R.L. (2004). Origin of the neighboring residue effect on peptide backbone conformation. Proc. Natl. Acad. Sci. USA *101*, 10967–10972.
51. Headlam, M.J., Wilce, M.C.J., and Tuckey, R.C. (2003). The F-G loop region of cytochrome P450scc (CYP11A1) interacts with the phospholipid membrane. Biochim. Biophys. Acta *1617*, 96–108.
52. Yamamoto, H., Esaki, M., Kanamori, T., Tamura, Y., Nishikawa, S.i., and Endo, T. (2002). Tim50 is a subunit of the TIM23 complex that links protein translocation across the outer and inner mitochondrial membranes. Cell *111*, 519–528.
53. Black, S.M., Harikrishna, J.A., Szklarz, G.D., and Miller, W.L. (1994). The mitochondrial environment is required for activity of the cholesterol side-chain cleavage enzyme, cytochrome P450scc. Proc. Natl. Acad. Sci. USA *91*, 7247–7251.
54. Omelchuk, O.A., Malyshev, V.I., Medvedev, M.G., Lysenkova, L.N., Belov, N.M., Dezhenkova, L.G., Grammatikova, N.E., Scherbakov, A.M., and Shchekotikhin, A.E. (2021). Stereochemistries and biological properties of oligomycin A Diels–Alder adducts. J. Org. Chem. *86*, 7975–7986.
55. Su, H., Wang, B., and Shaik, S. (2019). Quantum-mechanical/molecular-mechanical studies of CYP11A1-catalyzed biosynthesis of pregnenolone from cholesterol reveal a C-C bond cleavage reaction that occurs by a

compound I-mediated electron transfer. J. Am. Chem. Soc. *141*, 20079–20088.

56. Walther, D.M., Papic, D., Bos, M.P., Tommassen, J., and Rapaport, D. (2009). Signals in bacterial beta-barrel proteins are functional in eukaryotic cells for targeting to and assembly in mitochondria. Proc. Natl. Acad. Sci. USA *106*, 2531–2536.
57. Feldman, D.E., and Frydman, J. (2000). Protein folding in vivo: the importance of molecular chaperones. Curr. Opin. Struct. Biol. *10*, 26–33.
58. Bose, H.S., Lingappa, V.R., and Miller, W.L. (2002). Rapid regulation of steroidogenesis by mitochondrial protein import. Nature *417*, 87–91.
59. Pace, C.N. (1986). Determination and analysis of urea and guanidine hydrochloride denaturation curves. Methods Enzymol. *131*, 266–280.
60. Prasad, M., Pawlak, K.J., Burak, W.E., Perry, E.E., Marshall, B., Whittal, R.M., and Bose, H.S. (2017). Mitochondrial metabolic regulation by GRP78. Sci. Adv. *3*, e1602038.
61. Prasad, M., Kaur, J., Pawlak, K.J., Bose, M., Whittal, R.M., and Bose, H.S. (2015). Mitochondria-associated endoplasmic reticulum membrane (MAM) regulates steroidogenic activity via steroidogenic acute regulatory protein (StAR)-voltage-dependent anion channel 2 (VDAC2) interaction. J. Biol. Chem. *290*, 2604–2616.
62. Prasad, M., Walker, A.N., Kaur, J., Thomas, J.L., Powell, S.A., Pandey, A.V., Whittal, R.M., Burak, W.E., Petruzzelli, G., and Bose, H.S. (2016). Endoplasmic reticulum stress enhances mitochondrial metabolic activity in mammalian adrenals and gonads. Mol. Cell Biol. *36*, 3058–3074.
63. Bose, M., Whittal, R.M., Miller, W.L., and Bose, H.S. (2008). Steroidogenic activity of StAR requires contact with mitochondrial VDAC1 and phosphate carrier protein. J. Biol. Chem. *283*, 8837–8845.
64. Bose, H.S., and Doetch, N.E. (2023). Protocol for direct measurement of stability and activity of mitochondria electron transport chain complex II. STAR Protoc. *4*, 101996.
65. Lan, H.C., Li, H.J., Lin, G., Lai, P.Y., and Chung, B.C. (2007). Cyclic AMP stimulates SF-1-Dependent CYP11A1 expression through homeodomain-interacting protein kinase 3-mediated Jun N-terminal kinase and c-Jun phosphorylation. Mol. Cell Biol. *27*, 2027–2036.

STAR★METHODS

KEY RESOURCES TABLE

REAGENT or RESOURCE	SOURCE	IDENTIFIER
P450scc (CYP11A1) antibody	Dr. Bon-chu Chung	Ref: Mol Endocrinol 22:915–923, 2008
VDAC2 antibody	Home made	Ref: J Biol Chem 290, 2604–2616, 2015
Calnexin antibody	Santa Cruz Biotechnology	sc-23954
Tim23 antibody	Santa Cruz Biotechnology	sc-47724
Tim50 antibody	Santa Cruz Biotechnology	sc-365466 & sc-11414
GRP78 antibody	Santa Cruz Biotechnology	sc-53472 & sc-13539
Normal Rabbit IgG	Millipore Sigma	12–370
Mitochondria	Homemade	*Ref: STAR Protoc* 4, 101996 (2023)
Mitoplast	Homemade	*Ref: STAR Protoc* 4, 101996 (2023)
Rat testis	Mercer University	IACUC # A1707013 (Dr. Z-Q Zhao)
Sucrose	FISHER SCIENTIFIC	84097
HEPES	SIGMA	H3375
EGTA	CALBIOCHEM/SIGMA	324628
Na_2HO_4	FISHER SCIENTIFIC	S375-500
KH_2PO_4	FISHER SCIENTIFIC	P380-12
NaCl	FISHER SCIENTIFIC	AC447302500
KOH	FISHER SCIENTIFIC	501118107
ATP	SIGMA	A26209
Trilostane	SIGMA	SML 0141
Carbonyl Cyanide *m*-Chlorophenylhydrazone (mCCCP)	Calbiochem	555-60-2
Oligofectamine	Thermo Fisher	12252011
Lipofectamine	Invitrogen (Thermo Fisher)	18324-012 (New number 15338030)
β-mercaptoethanol	Calbiochem	60-24-2
DTT	SIGMA	D9779
PMSF	Millipore Sigma	329-98-6
Protease Inhibitor Cocktail	Thermo Fisher	J61852.XF
EDTA	Thermo Fisher Scientific	147865000
Acrylamide	BioRad	1610107
Bis Acrylamide	BioRad	1610201
SDS	BioRad	1610302
Tris HCl [tris(hydroxymethyl)] aminomethane hydrochloride	VWR (JT Baker)	JT4107-05
Tris (hydroxymethyl)aminomethane	VWR (JT Baker)	JT4102-05
Urea	Fisher Scientific	169–500
Valinomycin	Sigma-Aldrich	2001-95-8
Atractoloside	Sigma-Aldrich	17754-44-8
Oligomycin	Sigma-Aldrich	1404-19-9
4-(2-aminoethyl)benzenesulfonyl fluoride hydrochloride (AEBSF)	Gold Biotechnology	A-540-500
Sorbitol	Millipore Sigma	S1876
^{32}S Methionine	MP Biomedicals	C15100614
Protein A-Sepharose CL 4B Beads	GE-Healthcare	17-780-01

(*Continued on next page*)

Continued

REAGENT or RESOURCE	SOURCE	IDENTIFIER
Triton X-100	Millipore Sigma	T8787
Lubrol	MP Biomedicals	02195299-CF
Sodium deoxycholate	Millipore Sigma	30970
Radioimmunoassay (RIA) Kit	MP Biomedicals	07170102
Quick Start Bradford 1X Dye	BIO-RAD	5000205
Rabbit Reticulocyte Lysate	Promega	L4600
Protease Inhibitor Cocktail Set	Calbiochem	539132
Chemiluminescent Reagent	Thermo Fisher	34579
pSP64 -Vector	Promega	P1241
pCMV4 -Vector	Stratagene	211174
StAR cDNA	Home made	Ref: PNAS 92: 4778,1995
Cytochrome P450 side chain cleavage enzyme (SCC) cDNA	Dr. Walter Miller	Ref: PNAS 83: 8962, 1986
Ferredoxin cDNA	Dr. Walter Miller	Ref: PNAS 91: 7247, 1994
Ferredoxin reductase cDNA	Dr. Walter Miller	Ref: PNAS 91: 7247, 1994
pcDNA™3.1 Mammalian Expression Vector	Thermo Fisher Scientific	V79020
F2 (Cytochrome P450scc-Ferredoxin reductase-Ferredoxin) vector cDNA	Dr. Walter Miller	Ref: PNAS 91: 7247, 1994
Human dihydrofolate reductase (DHFR) cDNA	Dr. Gordon C. Shore	Ref: J Bio Chem 265:9444-9451, 1990
Glycerol Buffer	This paper	NA
Mitochondria Isolation Buffer	Home made	*Ref: STAR Protoc* 4, 101996 (2023)
Lysis Buffer	Home made	Ref: JBC 283: 8837–8845, 2008.
Urea - MA-10 Media	This paper	NA
E. coli DH 5α	Invitrogen (Thermo-Fisher)	34210 (Now EC0111)
COS-1	ATCC	CV-1 CCL-70
MA-10	ATCC	CRL-3050
Rat testicular tissue	Mercer University (to Dr. Z-Q Zhao)	IACUC # A1707013

RESOURCE AVAILABILITY

Lead contact

Further information and requests for resources and reagents should be directed to and will be fulfilled by the Lead Contact, Himangshu S Bose (bose_hs@mercer.edu).

Materials availability

This study did not generate any new unique reagents. Reagent request will be made readily fulfilled following materials transfer policies of Mercer University School of Medicine.

Data and code availability

- This study did not generate any new computational program or sequence data.
- This study did not generate any new code.
- Any additional information required to reanalyzes the data reported in this paper is available form the lead contact upon request.

EXPERIMENTAL MODEL AND SUBJECT DETAILS

MA-10 and COS-1 cells were purchased directly from ATCC. Mercer University checks mycoplasma contamination usually in every six months. The investigators are immediately informed once a contamination is detected in the individual laboratory. We have not received any report for our laboratory on mycoplasma contamination on these cells.

Plasmid construction, cell culture, mitochondria isolation and transfection

Plasmid construction

For subcloning and building of different constructs, human SCC (CYP11A1) cDNA was used as the template for PCR with specific combinations of sense and antisense primers.[23] Each of the constructs were sequenced to confirm the accuracy of each clone.

Cell Culture

Mouse Leydig MA-10 cells were cultured in Waymouth media (ThermoFisher/Invitrogen, Carlsberg, CA) in the presence of 1× L-Glutamine, 1X Gentamycin, 10% horse serum, and 5% fetal bovine serum (FBS). For urea-induced unfolding studies, dry Waymouth media (Sigma, St. Louis, MO) was solubilized in water containing urea to a final concentration of 2M, adjusted pH to 7.4, supplemented with 1× L-Glutamine, 1× Gentamycin, 10% horse serum, 5% fetal bovine serum and sterilized through a 0.22-micron filter under the tissue culture hood. To avoid formation of urea degradation product,[59] the urea-containing media was always freshly prepared prior to each experiment and never stored. Monkey kidney (COS-1) cells were cultured in Dulbecco's Modified Eagle's medium with high glucose supplemented with 10% FBS and penicillin-streptomycin. To avoid any endogenous steroidogenic activity from MA-10 cells, we performed all transfection experiments in nonsteroidogenic COS-1 cells[60,61] via Lipofectamine or Oligofectamine (Thermo Fisher).[60,62,63] As an inhibitor of 3β-hydroxysteroid dehydrogenase 2, we also incubated with 100 ng/mL trilostane (Sigma, MO, USA). For wild-type or mutated SCC transfection and activity analysis, COS-1 cells were plated at a density of 1 × 10^6 cells in 6-well plates 24 h prior to transfection followed by co-transfection with 1.0 μg of StAR, Ferredoxin and Ferredoxin reductase with[63] Lipofectamine (Invitrogen, Carlsbad, CA, USA). COS-1 cells do not express the P450scc steroidogenic system, so StAR was included to drive cholesterol transport from the outer to inner mitochondria. Ferredoxin reductase and Ferredoxin was also added to maintain the complete electron transport chain system to catalyze conversion of cholesterol to pregnenolone. The cells were washed with serum-free medium 12 h after transfections and supplemented with medium containing antibiotics (1X Pen/Step) and 10% serum. The medium was collected after 48 h, and the accumulated pregnenolone was measured from the media collected by radioimmunoassay (RIA kit, MP Biomedicals, Solon, OH, USA).

METHOD DETAILS

Isolation of mitochondria and activity

Immediately after the sacrifice, sheep adrenal and placenta were collected from the University of Florida Veterinary School, and mitochondria were isolated from tissues by differential centrifugation as described previously.[63,64] Mitochondrial pellets were resuspended in a 1:1 mix buffer on ice and incubated with 10 mM HEPES (pH 7.4) for 5 min. Mitoplasts were prepared by solubilizing the OMM in 1.2% (w/v) digitonin. Mitochondria were centrifuged at 10,000 ×g for 20 min. The OMM fraction was centrifuged at 130,000 ×g for 1 h to separate unimported SCC from the pellet membranes. IMM and matrix fractions were prepared by treating mitoplasts with 0.16 mg of non-ionic lubrol per mg of mitochondria followed by ultracentrifugation at 130,000 ×g for 1 h. The soluble fraction was referred to as the matrix, and the insoluble fraction as the IMM, although it should be noted that this fraction also contains some intermembrane space (IMS) components. The matrix fraction (supernatant) was removed, and the membrane pellet was resuspended in 1:1 mix buffer and kept on ice. The volume of the supernatant was measured, and the membrane pellet was resuspended in 1:1 mix buffer.[63,64]

Testes from our experimental animals were collected immediately after sacrifice, diced in an ice-cold mitochondria isolation buffer containing 250 mM sucrose, and separated by centrifugation at 3000 rpm. The supernatant was then centrifuged at 10,000 rpm. The pellet was processed for mitochondria purification or separation of compartmental fragmentation as described for the MA-10 cells.[60,61] The animal procedures for using rat adrenal or testes were approved by the institutional review board [Institutional Animal Care and Use Committee (IACUC) no. A1707013]. Mitochondria (2 g of protein) from the sheep adrenals, placenta and MA-10 cells were resuspended in a final volume of 100 of bioassay buffer (125 mM sucrose, 80 mM KCl, 5 mM $MgCl_2$, 10 mM NaH_2PO_4, 10 mM isocitrate, 25 mM HEPES, 0.1 mM ATP, and 10 mg/mL cholesterol, pH 7.4), as described before. Supernatants were then assayed for pregnenolone by radioimmunoassay.[10] Heat inactivated mitochondria was applied as a negative control.

In vitro synthesis and processing of the precursor protein with different mitochondrial fractions

Full-length precursor CYP11A1 (SCC) or the chimeric cDNA constructs fused with full-length 186-amino acid dihydrofolate reductase (DHFR) were subcloned in an SP6 vector,[8] translated in a cell-free rabbit reticulocyte system (CFS) in the presence of ^{35}S-labeled methionine following the manufacturer's instructions (Promega). Freshly isolated mitochondria or mitochondrial fractions were incubated with the ^{35}S-labeled precursor SCC. Ribosomes and their associated polypeptide chains were removed by centrifugation at 150,000 ×g for 15 min at 4°C.[9] Partial proteolysis was performed with proteinase K (PK) and trypsin independently with varying concentrations from 10 μg to 250 μg. An equal volume of matrix and membrane fractions was used in each reaction. As the membrane pellet was resuspended in an equal volume as that of the matrix fraction (supernatant), the amount of each fraction added to a processing reaction represents the ratio found in the mitochondria. For membrane integration analysis, Na_2CO_3 (100 mM) was freshly prepared prior to each experiment. The reaction was stopped by addition of equal volume of 2× SDS sample buffer followed by boiling in a water bath for 10 min. The samples were analyzed by SDS-PAGE, fixed in methanol/acetic acid (40:10), dried, and exposed to a phosphorimager screen (digital autoradiography; Molecular Dynamics/GE-Healthcare) or an X-ray film.

Urea unfolding

For all unfolding experiments various concentrations of urea were prepared in 1× import buffer[64] and incubated with the ^{35}S-SCC for 1 h prior to import experiments with the freshly isolated mitochondria from MA-10 cells. Urea import buffer was freshly prepared prior to each experiment. The import reactions were performed for 2 h at 26°C and analyzed as described above.

Western blot analysis

Purified protein or total cell lysate (12.5 μg) was separated by 12.5% SDS-PAGE and transferred to a polyvinylidine difluoride membrane (Millipore, Billerica, MA, USA). After blocking with 3% nonfat dry milk for 45 min, the membranes were probed overnight with primary antibodies (SCC, VDAC2, Tim23, Tim50, Calnexin and HSP70) at 4°C, and then incubated with the horseradish peroxidase-conjugated goat anti-rabbit IgG, anti-mouse IgG, or anti-donkey IgG (Pierce, Rockford, IL, USA) as needed. The primary antibodies specific for Tim23, Tim50, and HSP70 (Santa Crutz Biotechnology, Dallas, TX) were diluted 1: 200. Antibodies specific for calnexin and GRP78 (AbCam, Cambridge, UK) were diluted 1:3000; VDAC2 antibody was homemade[61] (1: 2000), and SCC antibody (1:3000) was a kind gift from Dr. Bon-Chu Chung.[65] Signals were developed with a chemiluminescent reagent (West Pico, Thermo Fisher) and exposed on an X-ray film.

Co-immunoprecipitation (co-IP) analysis

Tim50, SCC, Tim23, GRP78 and VDAC2 antibodies were independently pre-incubated with protein A-Sepharose CL 4B (0.5 μg/μL, Thermo Fisher/Amersham Biosciences, Sweden) in 100 μL of 1× co-IP buffer (1% Triton X-100, 200 mM NaCl and 0.5% sodium deoxycholate). After mixing for 2 h at 4°C, the beads were washed with at least 1× co-IP buffer five times and then incubated again with pure rabbit IgG control antibody (Sigma) for 1 h. After another wash series, freshly isolated mitochondrial pellets (25 mg/sample) were resuspended with ice-cold lysis buffer (20 mM Tris HCl, pH 8.0, 137 mM NaCl, 10% glycerol, 1% Triton X-100, 2 mM EDTA) at 4°C for 15 min. Insoluble material was removed by ultracentrifugation (30 min at 100,000 ×g). The supernatants were incubated overnight at 4°C in the presence of antibodies prebound to protein A Sepharose beads. After washing with 1× co-IP buffer and 10 mM HEPES (pH 7.4), the protein A-Sepharose pellets were resuspended and vortexed with 100 mM glycine (pH 3.0) for 10 s at 4°C. After addition of a pre-titrated volume of 1.0M Tris (pH 9.5), the beads were separated from the soluble material by centrifugation at 2000 ×g for 2 min at 4°C. The supernatants (immune complexes) were analyzed by Western blotting.

Transmission electron microscopy (TEM)

After 24 h following splitting the MA-10 cells, the media was replaced with freshly prepared Waymouth media containing 2M urea for additional 24 h, and the structure was visualized through live cell imaging (Nikon X100 magnification) and compared with untreated cells. Next, untreated and urea-treated cells (6×10^6) were washed twice with Phosphate Buffer Saline (PBS) at room temperature, gently scraped in the presence of PBS, and transferred to 50 mL plastic disposable Corning tubes. After centrifugation at 3500 rpm (Beckman Allegra 22R and rotor F630) for 10 min, the cells were fixed in 4% paraformaldehyde and 0.2% glutaraldehyde in 0.1M sodium cacodylate buffer, pH 7.4, dehydrated with a graded ethanol series through 95% and embedded in LR white resin. Thin sections of 75 nm thickness were cut with a diamond knife on a Leica EM UC6 ultramicrotome (Leica Microsystems, Bannockburn, IL, USA) and collected on 200 mesh nickel grids. The sections were blocked in 0.1% BSA in PBS for 4 h at room temperature (26°C) in a humidified atmosphere and incubated with SCC (1:2000) antibody in 0.1% BSA overnight at 4°C. Room temperature was 26°C unless otherwise stated. The sections were washed with PBS and floated on drops of anti-primary specific ultrasmall (<1.4 nm) Nanogold reagent (Nanoprobes, Yaphank, NY, USA) diluted 1:2000 in 0.1% BSA in PBS for 2–4 h at room temperature. After PBS and deionized H_2O washes, the sections were incubated with HQ Silver (Nanoprobes) for 8 min for silver enhancement, followed by washing in deionized H_2O. All sections were observed in a JEM 1230 transmission electron microscope (JEOL USA, Peabody, MA, USA) at 110 kV and imaged with an UltraScan 4000 CCD camera and First Light Digital Camera Controller (Gatan, Pleasanton, CA, USA).

Proteolytic digestion experiments

Proteolytic digestion experiments were performed at 4°C using various concentrations of PK in the presence and absence of 0.5% of Triton X-100. The reactions were terminated by the addition of an equal volume of 2× SDS sample buffer containing 2 mM PMSF and then incubating in a boiling water bath for 10 min. After electrophoresis, the samples were processed for Western blotting.

QUANTIFICATION AND STATISTICAL ANALYSIS

The data were analyzed using Kalidagraph or Microsoft Excel program and reported as mean ± standard error. Each experiment was performed at least in triplicate three different times and indicated in the figure legend. To compare quantitated images, we used one-way ANOVA. The *p*-values generated from each set of statistical tests were considered statistically significant at $p < 0.05$; the highest of the *p*-values are reported.

Statistical analysis

We have indicated in the individual figure legends of the means plus standard errors of the means (SEM) for three independent experiments performed at least three different times. The *p* value is also presented in the figure legends.